Journal of Molecular Spectroscopy 289 (2013) 35–40

Contents lists available at SciVerse ScienceDirect

Journal of Molecular Spectroscopy

journal homepage: www.elsevier.com/locate/jms

Analysis of a tritium enhanced water spectrum between 7200 and 7245 cm^{-1} using new variational calculations

Michael J. Down [a], Jonathan Tennyson [a,*], Masanori Hara [b], Yuji Hatano [b], Kaori Kobayashi [c]

[a] Department of Physics and Astronomy, University College London, London WC1E 6BT, UK
[b] Hydrogen Isotope Research Center, University of Toyama, 3190 Gofuku, Toyama-City, Toyama 930-8555, Japan
[c] Department of Physics, University of Toyama, 3190 Gofuku, Toyama-City, Toyama 930-8555, Japan

ARTICLE INFO

Article history:
Received 6 April 2013
In revised form 15 May 2013
Available online 13 June 2013

Keywords:
Vibration–rotation spectroscopy
Water
Infrared

ABSTRACT

A tritium enhanced water absorption spectrum previously recorded in the 7200–7245 cm^{-1} region is analysed. Variational calculations for HTO predict absorption to be dominated by the $2\nu_3$ vibrational band in this region. New assignment are made for HTO based on this line list with a band origin measured to be at 7236.03 cm^{-1}. A calculated T_2O line list predicts absorption in this region to be below the experimental detection limit despite the large quantity of tritium present. From 170 lines observed 37 known $H_2{}^{16}O$ lines are identified and 111 new HTO assignments are made.

1. Introduction

The heavy radioactive tritium (^3H) isotope of hydrogen has a half life of approximately 12.32 years [1]. It forms several isotopologues of water the most common being the singly substituted $HT^{16}O$ and the doubly substituted $T_2{}^{16}O$ which have trace natural abundances (see Table 1 below). Whilst sharing similar properties to $H_2{}^{16}O$, both form corrosive liquids due to self radiolysis and are highly toxic.

As radioactive water isotopologues, these species have been widely used as tracers in life science water transport studies including Refs. [2–5] to name but a few. Their radioactivity has also been put to use in the dating of water based liquids including vintage wines [6]. Rare isotopologue abundances have also often been used to trace atmospheric processes since isotopic variations can be caused by specific atmospheric drivers such as cometary and meteorite deposits at the top of the atmosphere. The spectra of these species are therefore of some importance to these communities, as they provide an opportunity for isotopologue specific detection.

Understanding and controlling tritium and the molecules it forms is also key in nuclear physics. In particular the harmful nature of tritiated water make its detection indispensable. High resolution spectroscopy provides a means of detecting tritiated water species with several benefits, including the potential for *in situ* real time observation and the ability to make observations without direct sampling.

Furthermore, documenting the spectra of these species is of value to the theoretical community [7], in their attempt to understand the breakdown of the Born Oppenheimer (BO) approximation. Recorded spectra of these species provide an important tool for evaluating *ab initio* non BO calculations, designed to model the breakdown of the BO approximation.

Previous high resolution studies of these isotopologues are limited to a handful of works [8–15]. Unlike stable water isotopologues only the fundamentals of these tritiated species have been previously observed at high resolution. Prior to these works Staats et al. [16] recorded near-infrared spectra for these species at significantly lower resolution. Rovibrational assignments are documented by Refs. [12,13,11,10], for the fundamentals and by Refs. [8,9] for pure rotational spectra. As an aid to new assignments new line lists for HTO and T_2O were hence computed as part of this work.

In this work we analyse a water spectrum recorded by Kobayashi et al. [17], expected to contain a mixture of H_2O, HTO and T_2O. The 7200–7245 cm^{-1} region studied has not previously been used to probe HTO and T_2O. We present new rotational assignments for HTO, dominated by the $2\nu_3$ vibrational band, and the new line lists for HTO and T_2O which we hope to contribute to future analyses.

The paper is structured as follows. The experimental data is described in Section 2. Section 3 presents a theoretical prediction of the observed spectrum according to approximate concentrations, including the new calculations. The techniques used in the analysis are described briefly in Section 4 and the results of the analysis and our new assignments are discussed in Section 5. Data

* Corresponding author.
E-mail address: j.tennyson@ucl.ac.uk (J. Tennyson).

0022-2852/$ - see front matter © 2013 Elsevier Inc. All rights reserved.
http://dx.doi.org/10.1016/j.jms.2013.05.016

Table 1
Experimental (Expt.) and natural abundances for the three dominant water isotopologues present in the gas mixture of Kobayashi et al. [20]. The experimental abundances are estimated statistically based on the relative intensities of $H_2{}^{16}O$ and $HT^{16}O$ assignments.

Isotopologue	Expt.	Natural
$H_2{}^{16}O$	0.01	0.997317
$HT^{16}O$	0.16	4.987×10^{-17}
$T_2{}^{16}O$	0.83	6.235×10^{-34}

sets arising from this work have been placed in the Supplementary Data.

2. The observed spectrum

Kobayashi et al. [17] recorded a frequency modulation near-infrared spectrum at 296 K scanning the 7200–7245 cm^{-1} spectral region containing some 170 line positions, with a resolution of 0.02 cm^{-1} and estimated precision of 0.003 cm^{-1}. The relative intensity limit of detectable lines is thought to be only around 10^{-2} times the strongest line, which places some limitation on the analysis. It should be noted that the spectral resolution does not limit the precision of line positions except in the case of blended lines. Although strong lines are well determined, having line widths (FWHM) of the order 0.02 cm^{-1} the presence of strong air moisture absorption lines reduces the reliability of intensity measurements and limits the sensitivity in those regions.

The gas chamber was filled with tritiated water produced using the technique described in the previous work of Marr et al. [18], and had an unknown ratio of [H]/[T]. Since deuterium and the rare oxygen isotopologues occur at natural abundances we expect the presence of $HT^{16}O$, $T_2{}^{16}O$, $H_2{}^{16}O$ to dominate the spectrum. Table 1 gives the abundance of the different isotopomers in the sample.

3. Predicted spectrum

Initial analysis made assignments using the HITRAN line list for $H_2{}^{16}O$ and an HTO line list available on-line at the Tomsk web address `http://spectra.iao.ru/`, based on the Partridge and Schwenke (PS) potential energy surface [19]. These line lists have the benefit that they are fully labelled with the usual vibrational normal mode and asymmetric top quantum numbers for water. Indeed, these assignments indicate the spectrum to be dominated by the $2\nu_3$ band in this region as expected. However the nearby $\nu_1 + \nu_2 + \nu_3$ and $2\nu_1 + 2\nu_2$ bands also contribute. No assignments of $T_2{}^{16}O$ using an equivalent line list were made.

These preliminary assignments indicate a ratio [HTO]/[H_2O)] ≈ 20, based on comparison I_{obs}/I_{calc} values for assignments to the two species. Based on purely statistical arguments and ignoring fractionation effects or any radiation induced chemistry this translates to the approximate concentrations for the three species given in Table 1. The corresponding ratio [T]/[H] ≈ 10.

Due to the lack of documented line lists for the two tritiated species our own variational calculations were undertaken based on the DVR3D program suite [21]. For each of these isotopologues calculations were undertaken up to $J_{MAX} = 15$ using Radau coordinates and an atomic mass for tritium taken from NIST [22]. Full 296 K line lists in the 0–10 000 cm^{-1} range are included in the Supplementary Material. In both cases intensities were calculated using the LTP2011 DMS of Lodi et al. [23].

For HTO the PES of Voronin et al. was used [24], with parameters based on their calculations for HDO [25], which were fully converged up to 20 000 cm^{-1}. For T_2O the PES of Shirin et al. [26] was used and parameters were based on their work for the $D_2{}^{16}O$ isotopologue [26] for which convergence in this region was fully tested. Although mass specific non Born–Oppenheimer contributions to the PES were originally introduced, the fundamental band origins were not improved, and the original PES was used without alteration. Fig. 1 presents an overview of our new line lists.

Fundamental band origins were in general agreement with previously observed values [7] for both of these line lists, as seen in Table 2. Partition functions were calculated based on the computed energy levels and were in general agreement with those available at Tomsk on line, once allowance is made for different conventions for the treatment of nuclear spin, with $Q_{HTO} = 775.4$ and $Q_{T_2O} = 785.1$ at 296 K, including all nuclear spin factors.

The line lists were used to produce a predicted spectrum where intensities are scaled by the estimated concentrations. This is shown in Fig. 2. Absorption is thus expected to be dominated by HTO and H_2O, with the $2\nu_2$ band of HTO centred on this region. Although the gas mixture contains a high concentration of T_2O, we do not expect any absorption for this region as it falls between vibrational bands. The strongest T_2O lines can be seen to be over 10^4 weaker than other strong lines in this region, and this is beyond the sensitivity of the experiment. This is confirmed by failure to assign T_2O lines to the spectrum using either our own calculations or the Tomsk PS line list (see Table 3).

Table 2
Comparison of observed and calculated band origins for the fundamental vibrational modes of HTO and T_2O. Both observed (Obs.) and calculated (Calc.) positions and their residuals Δ are in units of cm^{-1}.

	HTO			T_2O		
Band	Obs.	Calc.	Δ	Obs.	Calc.	Δ
ν_1	2299.8	2299.525	0.275	2237.2	2237.055	0.145
ν_2	1332.5	1332.431	0.069	995.4	995.360	0.040
ν_3	3716.6	3716.791	−0.191	2366.6	2366.568	0.032

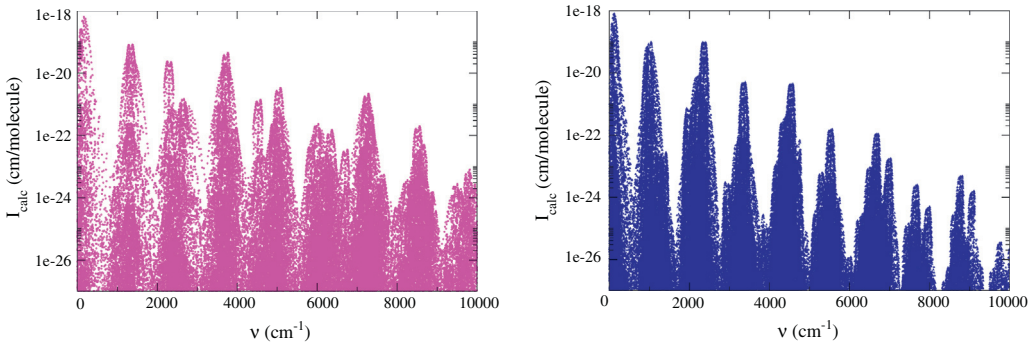

Fig. 1. Calculated line lists for HTO and T_2O in the 0–10 000 cm^{-1} range.

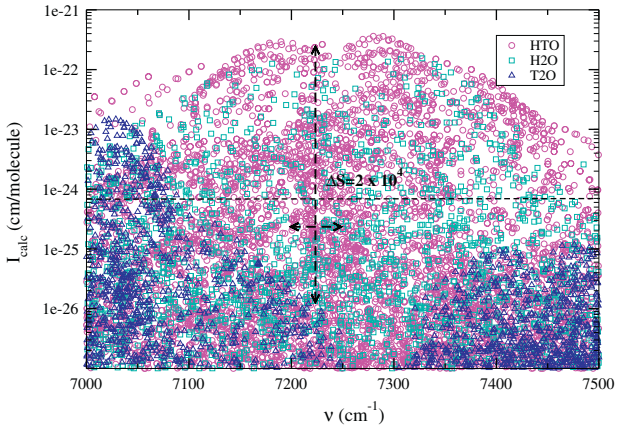

Fig. 2. Predicted line positions and intensities for the three isotopologues of water in the 7000–7500 cm^{-1} region. Intensities are scaled by the estimated experimental abundances given in Table 1. The horizontal arrow indicates the region in question whilst the vertical arrow indicates the difference between maximum HTO and T_2O intensities in that region. The horizontal dashed line indicates the intensity cut off used in the analysis.

4. Method

Our approach for assigning the previously unobserved lines in the spectrum is similar to previous work on a deuterated water spectrum [27], aiming first to identify and remove previously observed $H_2{}^{16}O$ lines from the experimental line list. This was done by comparison with the HITRAN database [28,29] which quotes position accuracy of 0.01–0.1 cm^{-1} in this region. However, as previously mentioned, there is no published data in this region for HTO.

While traditional methods of spectral analysis employ combination differences (CD's) as the major method for assigning spectra, new assignments were made by comparison with the line lists described in Section 3. There are several reasons for this approach. Primarily, the small spectral window available is unlikely to yield CD matches since P, Q and R branch transitions are unlikely to fall close together. Additionally, the lack of published experimental ground state energy levels, as required to calculate accurate CD's reduces the quality of this approach. Furthermore large line densities, the presence of multiple species in the spectrum and limited precision of the experimental data all increase the likelihood of false positive

Table 3
HTO assignments in the $2\nu_3$ band made using variational calculations performed as part of this work. Positions and residuals are also shown for equivalent assignments made using the calculations available on-line at the Tomsk web address `http://spectra.iao.ru/`, for the sake of comparison. ν_{obs}, ν_{calc}, ν_{Tomsk}, Δ, Δ_{Tomsk} and E″ are given in units of cm^{-1}, whilst I_{calc} are in units of cm/molecule. The units of observed intensity are arbitrary. Here the residuals are $\Delta = \nu_{obs} - \nu_{calc}$ and $\Delta_{Tomsk} = \nu_{obs} - \nu_{Tomsk}$. Lines marked with an asterisk are part of blended features.

ν_{obs}	ν_{calc}	ν_{Tomsk}	Δ	Δ_{Tomsk}	E″	I_{obs}	I_{calc}	I_{obs}/I_{calc}	J′	K_a'	K_c'	J″	K_a''	K_c''	
7200.680	7200.771	7200.689	−0.091	−0.009	114.576	372.5	8.173E−22	4.558E+23	3	1	3	4	0	4	
7200.887	7200.993	7200.977	−0.106	−0.090	591.369	64.9	2.481E−23	2.616E+24	8	3	5	7	4	4	
7201.231	7201.309	7201.239	−0.078	−0.008	69.188	484.7	1.640E−21	2.956E+23	2	0	2	3	0	3	
7201.703	7201.787	7201.716	−0.084	−0.013	81.695	524.9	1.371E−21	3.830E+23	2	1	2	3	1	3	
7201.904	7201.988	7201.912	−0.084	−0.008	202.009	306.2	9.447E−22	3.241E+23	5	0	5	5	1	4	
7202.494	7202.573	7202.531	−0.079	−0.037	266.677	35.3	6.853E−23	5.147E+23	5	2	4	4	3	1	
7203.562	7203.701	7203.945	−0.139	−0.383	934.939	14.1	2.505E−23	5.633E+23	9	5	5	9	5	4	*
7203.562	7203.710	7203.954	−0.149	−0.392	934.933	14.1	2.509E−23	5.625E+23	9	5	4	9	5	5	*
7206.521	7206.648	7206.537	−0.127	−0.016	499.924	16.2	7.070E−23	2.295E+23	8	2	7	8	2	6	
7208.253	7208.348	7208.264	−0.094	−0.010	202.009	31.8	1.185E−22	2.680E+23	5	1	5	5	1	4	
7208.438	7208.516	7208.447	−0.078	−0.010	140.563	460.7	1.213E−21	3.798E+23	4	0	4	4	1	3	*
7208.438	7208.516	7208.457	−0.078	−0.020	27.619	460.7	6.160E−22	7.479E+23	0	0	0	1	1	1	*
7209.636	7209.776	7209.716	−0.140	−0.080	684.490	37.4	1.125E−22	3.325E+23	8	4	5	8	4	4	
7209.855	7209.904	7209.848	−0.050	0.007	684.406	141.1	1.134E−22	1.244E+24	8	4	4	8	4	5	
7209.965	7210.208	7210.104	−0.244	−0.140	202.009	74.1	2.178E−22	3.401E+23	4	2	3	5	1	4	
7210.721	7210.879	7210.743	−0.159	−0.023	591.397	38.8	1.750E−22	2.218E+23	7	4	4	7	4	3	
7210.791	7210.882	7210.836	−0.091	−0.045	591.369	26.8	1.948E−22	1.377E+23	7	4	3	7	4	4	
7211.693	7211.805	7211.771	−0.113	−0.078	510.028	251.9	3.220E−22	7.822E+23	6	4	3	6	4	2	*
7211.693	7211.815	7211.780	−0.122	−0.088	510.020	251.9	3.224E−22	7.813E+23	6	4	2	6	4	3	*
7212.317	7212.396	7212.353	−0.079	−0.036	325.018	12.7	8.274E−23	1.535E+23	6	2	5	5	3	2	
7212.554	7212.662	7212.638	−0.108	−0.084	440.342	297.0	5.183E−22	5.731E+23	5	4	2	5	4	1	*
7212.554	7212.664	7212.640	−0.110	−0.086	440.340	297.0	5.184E−22	5.730E+23	5	4	1	5	4	2	*
7212.795	7212.871	7212.805	−0.076	−0.010	34.765	141.1	1.294E−21	1.091E+23	1	0	1	2	0	2	
7212.820	7212.901	7212.833	−0.081	−0.014	49.279	121.4	9.038E−22	1.343E+23	1	1	1	2	1	2	
7213.176	7213.254	7213.191	−0.078	−0.016	91.185	356.3	1.355E−21	2.629E+23	3	0	3	3	1	2	
7213.191	7213.220	7213.306	−0.029	−0.116	394.820	3.5	1.018E−23	3.465E+23	3	1	3	2	2	0	
7213.297	7213.401	7213.387	−0.104	−0.089	382.311	601.1	8.191E−22	7.339E+23	4	4	1	4	4	0	
7213.297	7213.401	7213.387	−0.104	−0.089	382.310	601.1	8.191E−22	7.339E+23	4	4	0	4	4	1	
7213.565	7213.728	7213.595	−0.163	−0.031	402.088	28.9	7.303E−23	3.961E+23	6	3	4	7	2	5	
7214.008	7214.162	7214.051	−0.154	−0.043	678.615	67.0	5.777E−23	1.160E+24	9	3	7	9	3	6	
7214.202	7214.294	7214.218	−0.093	−0.016	69.188	261.1	6.172E−22	4.230E+23	2	1	2	3	0	3	
7214.371	7214.458	7214.442	−0.087	−0.071	684.406	34.6	2.004E−23	1.725E+24	9	3	6	8	4	5	*
7214.371	7214.486	7214.389	−0.116	−0.018	402.088	34.6	1.267E−22	2.729E+23	7	2	6	7	2	5	*
7215.795	7215.651	7215.530	0.144	0.265	678.615	16.9	2.450E−23	6.912E+23	8	4	5	9	3	6	*
7216.391	7216.467	7216.408	−0.076	−0.017	54.029	558.8	1.267E−21	4.412E+23	2	0	2	2	1	1	
7217.022	7217.113	7217.037	−0.092	−0.015	140.563	43.7	1.881E−22	2.326E+23	4	1	4	4	1	3	
7218.274	7218.433	7218.376	−0.159	−0.103	29.203	214.5	9.066E−22	2.366E+23	1	0	1	1	1	0	
7218.342	7218.508	7218.452	−0.166	−0.110	789.360	217.3	1.662E−23	1.307E+25	10	3	8	9	4	5	
7219.091	7219.223	7219.132	−0.132	−0.041	477.420	77.6	1.928E−22	4.025E+23	7	3	5	7	3	4	
7219.502	7219.728	7219.619	−0.226	−0.117	674.583	75.5	2.601E−23	2.902E+24	8	4	4	9	3	7	
7220.343	7220.418	7220.368	−0.075	−0.026	137.258	71.3	1.059E−22	6.727E+23	4	1	4	3	2	1	
7220.384	7220.487	7220.401	−0.104	−0.018	316.927	137.6	2.178E−22	6.316E+23	6	2	5	6	2	4	

(*continued on next page*)

Table 3 (*continued*)

ν_{obs}	ν_{calc}	ν_{Tomsk}	Δ	Δ_{Tomsk}	E''	I_{obs}	I_{calc}	I_{obs}/I_{calc}	J'	K'_a	K'_c	J''	K''_a	K''_c	
7220.468	7220.598	7220.514	−0.130	−0.047	395.218	156.6	3.289E−22	4.762E+23	6	3	4	6	3	3	
7221.277	7221.356	7221.308	−0.079	−0.031	395.218	21.2	7.858E−23	2.693E+23	7	2	6	6	3	3	
7221.413	7221.545	7221.467	−0.132	−0.054	325.018	207.4	5.415E−22	3.831E+23	5	3	3	5	3	2	*
7221.515	7221.650	7221.573	−0.135	−0.058	394.820	121.4	3.215E−22	3.775E+23	6	3	3	6	3	4	
7221.675	7221.815	7221.742	−0.140	−0.067	476.443	50.1	1.803E−22	2.779E+23	7	3	4	7	3	5	
7221.762	7221.897	7221.821	−0.135	−0.060	324.884	201.8	5.382E−22	3.750E+23	5	3	2	5	3	3	
7222.103	7222.224	7222.151	−0.121	−0.048	266.677	318.9	8.711E−22	3.661E+23	4	3	2	4	3	1	
7222.198	7222.312	7222.240	−0.115	−0.042	266.643	266.6	8.700E−22	3.065E+23	4	3	1	4	3	2	
7222.509	7222.644	7222.579	−0.136	−0.070	569.717	19.8	9.533E−23	2.072E+23	8	3	5	8	3	6	
7222.614	7222.729	7222.660	−0.114	−0.045	220.093	588.4	1.399E−21	4.207E+23	3	3	1	3	3	0	*
7222.614	7222.741	7222.672	−0.127	−0.058	220.089	588.4	1.398E−21	4.208E+23	3	3	0	3	3	1	*
7223.527	7223.594	7223.553	−0.067	−0.026	101.881	14.8	8.626E−23	1.718E+23	3	1	2	2	2	1	
7224.076	7224.162	7224.092	−0.086	−0.015	91.185	152.4	3.001E−22	5.079E+23	3	1	3	3	1	2	
7224.453	7224.508	7224.446	−0.055	0.007	11.627	382.4	7.236E−22	5.285E+23	0	0	0	1	0	1	
7224.674	7224.764	7224.685	−0.090	−0.011	244.486	132.6	3.615E−22	3.669E+23	5	2	4	5	2	3	
7225.615	7225.689	7225.635	−0.074	−0.020	184.668	38.1	1.097E−22	3.473E+23	5	1	5	4	2	2	
7225.759	7225.874	7225.777	−0.116	−0.018	140.563	34.6	1.670E−22	2.070E+23	3	2	2	4	1	3	
7227.331	7227.415	7227.343	−0.084	−0.012	34.765	83.3	3.331E−22	2.500E+23	1	1	1	2	0	2	
7227.453	7227.549	7227.476	−0.097	−0.023	184.668	173.6	5.848E−22	2.968E+23	4	2	3	4	2	2	
7228.703	7228.784	7228.724	−0.081	−0.021	244.486	33.2	8.711E−23	3.807E+23	6	1	6	5	2	3	
7229.201	7229.342	7229.436	−0.141	−0.235	317.105	39.5	3.825E−23	1.033E+24	6	2	4	7	1	7	
7229.373	7229.453	7229.387	−0.080	−0.015	54.029	145.3	5.021E−22	2.895E+23	2	1	2	2	1	1	
7229.484	7229.636	7229.515	−0.152	−0.031	316.927	16.2	7.499E−23	2.164E+23	5	3	3	6	2	4	
7229.922	7230.017	7229.949	−0.096	−0.027	101.992	605.4	1.574E−21	3.845E+23	2	2	1	2	2	0	
7230.168	7230.266	7230.198	−0.098	−0.030	101.881	396.5	1.574E−21	2.520E+23	2	2	0	2	2	1	
7231.072	7231.163	7231.097	−0.091	−0.025	183.039	103.0	5.832E−22	1.766E+23	4	2	2	4	2	3	
7231.664	7231.776	7231.669	−0.113	−0.006	495.022	12.0	8.894E−23	1.349E+23	11	3	8	11	3	9	*
7232.772	7232.832	7232.789	−0.060	−0.017	240.794	87.5	3.631E−22	2.409E+23	5	2	3	5	2	4	
7232.895	7232.976	7232.914	−0.081	−0.019	29.203	342.9	1.005E−21	3.411E+23	1	1	1	1	1	0	
7235.643	7235.746	7235.662	−0.103	−0.019	178.456	16.9	9.661E−23	1.753E+23	4	2	2	5	1	5	
7236.071	7236.113	7236.108	−0.042	−0.036	394.820	27.5	6.728E−23	4.090E+23	7	2	5	6	3	4	
7236.181	7236.252	7236.192	−0.071	−0.011	27.619	421.2	1.003E−21	4.201E+23	1	1	0	1	1	1	
7236.462	7236.583	7236.693	−0.121	−0.232	309.865	151.7	1.151E−22	1.318E+24	6	2	4	6	2	5	*
7236.546	7236.643	7236.568	−0.097	−0.023	1034.761	20.5	6.455E−24	3.170E+24	12	3	10	11	4	7	
7236.770	7236.916	7236.806	−0.146	−0.036	309.865	50.8	6.308E−23	8.053E+23	5	3	2	6	2	5	*
7237.737	7237.795	7237.757	−0.058	−0.020	136.706	54.3	1.744E−22	3.115E+23	4	1	3	3	2	2	
7239.198	7239.275	7239.216	−0.077	−0.018	49.279	299.2	4.980E−22	6.007E+23	2	1	1	2	1	2	
7239.586	7239.746	7239.666	−0.160	−0.080	678.615	37.4	2.575E−23	1.452E+24	10	2	9	9	3	6	*
7240.713	7240.806	7240.764	−0.093	−0.052	390.128	14.1	1.030E−22	1.370E+23	7	2	5	7	2	6	
7240.738	7240.825	7240.734	−0.087	0.004	91.185	24.0	8.683E−23	2.763E+23	2	2	1	3	1	2	
7242.810	7242.878	7242.828	−0.067	−0.018	27.619	28.0	3.449E−22	8.122E+22	2	0	2	1	1	1	

CD's. Lack of resolution in general exacerbates this problem, since estimated precisions are lower for blended lines. Conversely, the accuracy of computed line lists allows assignments to be made confidently by comparison with calculations.

Assignments are based upon a direct matching routine which compares positions of observed peaks and known or calculated line positions within a frequency interval, with the possibility of a constant frequency shift being applied. The chance that lines match coincidentally is deemed to be small for the line density of this spectrum and the small frequency intervals employed. The presence of a large number of matches found within a small frequency interval was used to determine an appropriate shift for each line list and the matching frequency range was then trimmed correspondingly to minimise the chance of coincidental matches. All assignments have also been verified using the Tomsk PS based line list described above, which provide the usual vibrational and rotational labels for water.

Assignments were also required to have consistent intensity agreement. Computed I_{obs}/I_{calc} ratios were used not only to determine approximate concentrations as discussed above, but also for validation of assignments, for which intensities should show consistent behaviour. This was limited by the uncertainties in the experimental relative intensity data.

Assignments have been checked using CD's, based on calculated energy levels, where possible. However, for the small numbers of lines involved few energy levels are associated to more than one observed line. As a result only 25 energy levels can be confidently derived. These are tabulated in Table 7.

5. Results and discussion

Initially, 37 $H_2{}^{16}O$ features were identified using HITRAN out of 68 HITRAN lines in the region above the intensity threshold of 1×10^{24} cm/molecule. Assignments were made within a 0.01 cm^{-1} window of the observed position except for two outliers, with errors less than 0.025 cm^{-1}. The small average shift of 0.0005 cm^{-1} observed is deemed to be below the experimental accuracy of this data. These lines were removed from the analysis, and are present in the Supplementary Material but will not be discussed further here.

In total 111 new features were assigned to HTO using our calculations, including 38 blended features, from the 183 lines with calculated intensity above the threshold. These belonged to three vibrational bands. Both blended features and outliers in terms of position and intensity agreement must be considered less reliable.

The new assignments were dominated by the strongest band, the $2\nu_3$ band, with the 83 assignments made including 20 blended features. An average band shift of −0.103 cm^{-1} was observed between the calculated and observed positions, and lines were assigned within 0.1 cm^{-1} of this value, except for one outlier with a 0.23 cm^{-1} residual. Table 3 shows these assigned lines; blended lines are clearly indicated.

A further 19 assignments were made to the next strongest band, the $\nu_1 + \nu_2 + \nu_3$ band, and are tabulated in Table 4. These show a large spread around an average shift of 0.043 cm^{-1}, with the standard deviation of residuals at 0.124 cm^{-1} and as such must be considered less reliable. This band also contains 7 blended features.

Table 4
HTO assignments in the $v_1 + v_2 + v_3$ band made using variational calculations performed as part of this work. Positions and residuals are also shown for equivalent assignments made using the calculations available on-line at the Tomsk web address `http://spectra.iao.ru/`, for the sake of comparison. v_{obs}, v_{calc}, v_{Tomsk}, Δ, Δ_{Tomsk} and E'' are given in units of cm^{-1}, whilst I_{calc} are in units of cm/molecule. The units of observed intensity are arbitrary. Here the residuals are $\Delta = v_{obs} - v_{calc}$ and $\Delta_{Tomsk} = v_{obs} - v_{Tomsk}$. Lines marked with an asterisk are part of blended features.

v_{obs}	v_{calc}	v_{Tomsk}	Δ	Δ_{Tomsk}	E''	I_{obs}	I_{calc}	I_{obs}/I_{calc}	J'	K'_a	K'_c	J''	K''_a	K''_c	
7201.107	7201.072	7201.176	0.035	−0.069	820.175	21.2	1.161E−23	1.824E+24	10	2	9	11	2	10	
7202.705	7202.728	7202.842	−0.023	−0.137	716.932	522.1	3.289E−23	1.588E+25	10	0	10	11	1	11	
7203.562	7203.451	7203.564	0.111	−0.002	716.209	14.1	4.319E−23	3.267E+23	10	0	10	11	0	11	*
7206.162	7206.215	7206.439	−0.053	−0.277	266.677	28.9	6.209E−23	4.659E+23	3	2	2	4	3	1	
7209.925	7209.980	7210.128	−0.056	−0.203	481.445	45.9	5.253E−23	8.731E+23	7	1	6	8	2	7	
7215.795	7215.637	7215.832	0.158	−0.037	905.592	16.9	8.342E−24	2.030E+24	9	4	6	10	4	7	*
7218.645	7218.524	7218.722	0.121	−0.077	600.711	19.1	4.930E−23	3.864E+23	9	1	9	10	0	10	
7218.730	7218.648	7218.880	0.082	−0.150	220.093	62.8	6.951E−23	9.034E+23	2	2	1	3	3	0	
7218.813	7218.781	7219.013	0.032	−0.200	220.089	37.4	6.956E−23	5.376E+23	2	2	0	3	3	1	
7220.498	7220.388	7220.646	0.110	−0.149	1050.746	19.1	2.422E−24	7.867E+24	9	5	4	10	5	5	*
7220.498	7220.399	7220.657	0.099	−0.160	1050.730	19.1	2.427E−24	7.849E+24	9	5	5	10	5	6	*
7221.413	7221.290	7221.444	0.123	−0.031	610.265	207.4	4.938E−23	4.201E+24	8	2	6	9	2	7	*
7227.037	7227.147	7227.260	−0.110	−0.223	496.822	17.6	9.153E−23	1.927E+23	8	0	8	9	1	9	
7231.664	7231.511	7231.697	0.153	−0.034	184.668	12.0	5.824E−23	2.059E+23	3	1	3	4	2	2	*
7234.865	7234.494	7234.680	0.371	0.185	240.794	64.9	7.263E−23	8.938E+23	4	1	3	5	2	4	
7239.133	7238.870	7238.975	0.263	0.158	680.789	60.7	8.084E−24	7.506E+24	10	0	10	10	1	9	
7239.586	7239.674	7239.844	−0.088	−0.258	481.445	37.4	7.499E−23	4.987E+23	7	2	6	8	2	7	*
7241.878	7241.990	7242.133	−0.112	−0.255	399.130	28.9	1.476E−22	1.960E+23	7	0	7	8	0	8	

Table 5
HTO assignments in the $2v_1 + 2v_2$ band made using variational calculations performed as part of this work. Positions and residuals are also shown for equivalent assignments made using the calculations available on-line at the Tomsk web address `http://spectra.iao.ru/`, for the sake of comparison. v_{obs}, v_{calc}, v_{Tomsk}, Δ, Δ_{Tomsk} and E'' are given in units of cm^{-1}, whilst I_{calc} are in units of cm/molecule. The units of observed intensity are arbitrary. Here the residuals are $\Delta = v_{obs} - v_{calc}$ and $\Delta_{Tomsk} = v_{obs} - v_{Tomsk}$. Lines marked with an asterisk are part of blended features.

v_{obs}	v_{calc}	v_{Tomsk}	Δ	Δ_{Tomsk}	E''	I_{obs}	I_{calc}	I_{obs}/I_{calc}	J'	K'_a	K'_c	J''	K''_a	K''_c	
7207.452	7207.249	7207.557	0.203	−0.105	738.177	106.5	7.466E−23	1.427E+24	7	5	3	7	5	2	*
7207.452	7207.249	7207.557	0.202	−0.105	738.176	106.5	7.467E−23	1.427E+24	7	5	2	7	5	3	*
7209.023	7208.794	7209.128	0.228	−0.105	657.196	52.2	1.221E−22	4.274E+23	6	5	2	6	5	1	*
7209.023	7208.794	7209.128	0.228	−0.105	657.196	52.2	1.222E−22	4.274E+23	6	5	1	6	5	2	*
7210.434	7210.156	7210.511	0.278	−0.077	587.803	36.0	1.947E−22	1.848E+23	5	5	0	5	5	1	*
7210.434	7210.156	7210.511	0.278	−0.077	587.803	36.0	1.947E−22	1.848E+23	5	5	1	5	5	0	*
7221.206	7220.982	7221.523	0.224	−0.317	360.209	7.8	1.061E−23	7.315E+23	8	1	7	7	1	6	
7236.770	7236.681	7237.237	0.089	−0.466	440.340	50.8	2.859E−23	1.777E+24	6	4	3	5	4	2	*
7236.770	7236.689	7237.244	0.082	−0.474	440.342	50.8	2.859E−23	1.777E+24	6	4	2	5	4	1	*

Table 6
Estimated HTO band origins for $2v_3$, $2v_1 + 2v_2$, and $v_1 + v_2 + v_3$ derived from this work, using calculated band origins and the average observed band shifts $\bar{\Delta}$, alongside the number and standard deviation σ of assignments in each band, all in units of cm^{-1}.

Band	Origin	$\bar{\Delta}$	σ	No. assigned	No. blended
$2v_3$	7236.07	−0.103	0.045	83	20
$2v_1 + 2v_2$	7129.67	0.201	0.059	9	8
$v_1 + v_2 + v_3$	7335.85	0.043	0.124	19	7

Tentative assignments to the $2v_1 + 2v_2$ band were also made and are shown in Table 5. These assignments showed an average shift of 0.201 cm^{-1} with a relatively small standard deviation of 0.059 cm^{-1}. Nearly all of these assignments belong to blended features and as such must again be considered less reliable.

The remaining 41 unassigned features are all weak with observed relative intensity less than 0.1. Such lines become hard to assign when low experimental accuracies combine with large band shifts for the calculated positions. While it is possible higher values of J in the computed line list could account for some of these features, it is thought to be unlikely for $J > 15$. Neither is it thought, as explained above, that any features belong to the T_2O species, for which similar analysis was unsuccessfully attempted. Any further assignments to this spectrum using the presently available data must at best be considered tentative.

Table 7
Energy levels and standard deviations σ derived from experimental positions and calculated lower energies using CD's. N denotes the number of transitions sharing the same upper state in each case. Please note for $N = 2$, σ corresponds to half the difference between the two derived energy values.

v_1	v_2	v_3	J	K_a	K_c	E (cm^{-1})	σ (cm^{-1})	N
0	0	2	0	0	0	7236.068	0.011	2
0	0	2	1	0	1	7247.518	0.042	2
0	0	2	1	1	1	7262.097	0.002	3
0	0	2	1	1	0	7263.793	0.007	2
0	0	2	2	0	2	7270.423	0.005	3
0	0	2	2	1	2	7283.396	0.005	3
0	0	2	3	1	3	7315.259	0.003	2
0	0	2	2	2	1	7331.918	0.005	2
0	0	2	4	1	4	7357.593	0.008	2
0	0	2	5	1	5	7410.273	0.010	2
0	0	2	4	2	3	7412.047	0.073	2
0	0	2	4	2	2	7414.105	0.006	2
0	0	2	5	2	4	7469.165	0.005	2
0	0	2	6	2	5	7537.323	0.012	2
0	0	2	6	2	4	7546.316	0.010	2
0	0	2	5	3	3	7546.421	0.010	2
0	0	2	5	3	2	7546.640	0.005	2
0	0	2	6	3	4	7615.670	0.017	2
0	0	2	7	2	6	7616.477	0.018	2
0	0	2	7	2	5	7630.866	0.025	2
1	1	1	7	0	7	7641.009	0.001	2
0	0	2	8	3	5	7792.241	0.015	2
0	0	2	8	4	4	7894.171	0.090	2
0	0	2	8	4	5	7894.268	0.142	2
1	1	1	10	0	10	7919.703	0.067	2

The assignments were used to produce estimates of experimental band origins for the three observed bands. These values shown in Table 6 were derived from the calculated band origins and the observed band shifts described above. Based on the number of assignments used only the $2\nu_3$ band origin should be considered reliable.

CD checks proved possible for 53 of the new assignments, comprising 25 upper energy levels. Agreement was found to be better than a standard deviation of 0.1 cm^{-1} in all cases, except two blended transitions. The large CD errors can in general be expected, as a result of using calculated lower energy levels and the low accuracy of the experiment, particularly for blended lines. The energy levels observed are presented in Table 7 and are included in the Supplementary Material.

The available PS based Tomsk line list provide more accurate positions in many, but not all cases, compared with the calculations made as part of this work. In particular positions calculated in this work were in general more accurate for the $\nu_1 + \nu_2 + \nu_3$ band. Intensities from the two sets of computations are of comparable quality.

6. Conclusions

Our analysis gives 111 new assignments to three different vibrational bands of HTO in the 7200–7245 cm^{-1} spectral region. Although there are many blended lines and the experimental accuracy is limiting, we consider the vast majority of the 83 presented $2\nu_3$ assignments to be thoroughly reliable and an important development in this region for HTO.

The sensitivity of the experiment did not allow detection of any T_2O features. Our line lists predicts this was due to the low T_2O intensities in the small spectral region employed, in a region dominated by HTO. Future experiments will need to exploit greater sensitivity and/or greater tritium concentrations in order to assign this species in this region.

The derived band origins presented here are the first inferred experimentally for HTO beyond the fundamentals. As such they should be of some value to the theoretical community.

We present the analysed spectrum as Supplementary Material, alongside the newly observed energy levels. The line lists computed for HTO and T_2O at 296 K, in the 0–10 000 cm^{-1} range are also included. These include all $J \leqslant 15$ transitions, and relative intensities greater than 10^{-12} times the strongest line. Considering the undocumented nature of the Tomsk line lists available on-line, we hope these line lists will prove a valuable resource in future analysis of tritiated water spectra.

Acknowledgments

Michael J Down thanks NERC for a studentship. This work is supported by ERC Advanced Investigator Project 267219. We also acknowledge the help of N.F. Zobov in attaining the D_2O PES employed here. Kaori Kobayashi is grateful for the financial support received from a Grant-in-Aid by the Ministry of Education, Culture, Sport, Science and Technology of Japan (18760635, 20049002) and the joint research program of the Hydrogen Isotope Research Center, University of Toyama.

Appendix A. Supplementary material

Supplementary data for this article are available on ScienceDirect (www.sciencedirect.com) and as part of the Ohio State University Molecular Spectroscopy Archives (http://library.osu.edu/sites/msa/jmsa_hp.htm). Supplementary data associated with this article can be found, in the online version, at http://dx.doi.org/10.1016/j.jms.2013.05.016.

References

[1] L. Lucas, M. Unterweger, J. Res. Natl. Inst. Stand. Technol. 105 (2000) 541–549.
[2] R.S. Bowman, Soil Sci. Soc. Am. J. 48 (1984) 987–993.
[3] F.M. Phillips, Soil Sci. Soc. Am. J. 58 (1994) 15–24.
[4] P.J. Wierenga, M.T. Van Genuchten, Ground Water 27 (1989) 35–42.
[5] S.C. Kalhan, J. Nutr. 126 (1996) S362–S369.
[6] S. Kaufman, W.F. Libby, Phys. Rev. 93 (1954) 1337–1344.
[7] N.F. Zobov, O.L. Polyansky, C.R. Le Sueur, J. Tennyson, Chem. Phys. Letts. 260 (1996) 381–387.
[8] F.C. De Lucia, P. Helminger, W. Gordy, H.W. Morgan, P.A. Staats, Phys. Rev. A 8 (1973) 2785–2791.
[9] P. Helminger, F.C. De Lucia, W. Gordy, P.A. Staats, H.W. Morgan, Phys. Rev. A 10 (1974) 1072–1081.
[10] S. Cope, D. Russell, H. Fry, L. Jones, J. Barefield, J. Molec. Spectrosc. 120 (1986) 311–316.
[11] S.D. Cope, D.K. Russell, H.A. Fry, L.H. Jones, J.E. Barefield, J. Molec. Spectrosc. 127 (1988) 464–471.
[12] H.A. Fry, L.H. Jones, J. Barefield, J. Molec. Spectrosc. 103 (1984) 41–55.
[13] O.N. Ulenikov, V.N. Cherepanov, A.B. Malikova, J. Molec. Spectrosc. 146 (1991) 97–103.
[14] R.A. Carpenter, N.M. Gailar, H.W. Morgan, P.A. Staats, J. Molec. Spectrosc. 44 (1972) 197–205.
[15] M. Tine, L.H. Coudert, in: Abstracts of OSU International Symposium on Molecular Spectroscopy 2000–2009. 2005-RE-11.
[16] P.A. Staats, H.W. Morgan, J.H. Goldstein, J. Chem. Phys. 24 (1956) 916–917.
[17] K. Kobayashi, T. Enokida, D. Iio, Y. Yamada, M. Hara, Y. Hatano, Fusion Sci. Technol. 60 (2011) 941–943.
[18] A.J. Marr, T.J. Sears, B.C. Chang, J. Chem. Phys. 109 (1998) 3431–3442.
[19] H. Partridge, D.W. Schwenke, J. Chem. Phys. 106 (1997) 4618–4639.
[20] J. Orphal, A.A. Ruth, Opt. Express 16 (2008) 19232–19243.
[21] J. Tennyson, M.A. Kostin, P. Barletta, G.J. Harris, O.L. Polyansky, J. Ramanlal, N.F. Zobov, Comput. Phys. Commun. 163 (2004) 85–116.
[22] G. Audi, A.H. Wapstra, C. Thibault, Nucl. Phys. A 729 (2003) 337–676.
[23] N.F. Zobov, S.V. Shirin, R.I. Ovsyannikov, O.L. Polyansky, S.N. Yurchenko, R.J. Barber, J. Tennyson, R. Hargreaves, P. Bernath, J. Mol. Spectrosc. 269 (2011) 104–108.
[24] S.N. Yurchenko, B.A. Voronin, R.N. Tolchenov, N. Doss, O.V. Naumenko, W. Thiel, J. Tennyson, J. Chem. Phys. 128 (2008) 044312.
[25] B.A. Voronin, J. Tennyson, R.N. Tolchenov, A.A. Lugovskoy, S.N. Yurchenko, Mon. Not. Roy. Astr. Soc. 402 (2010) 492–496.
[26] S.V. Shirin, N.F. Zobov, O.L. Polyansky, J. Quant. Spectrosc. Radiat. Transf. 109 (2008) 549–558.
[27] M.J. Down, J. Tennyson, J. Orphal, P. Chelin, A.A. Ruth, J. Molec. Spectrosc. 282 (2012) 1–8.
[28] J. Tennyson, P.F. Bernath, L.R. Brown, A. Campargue, M.R. Carleer, A.G. Császár, L. Daumont, R.R. Gamache, J.T. Hodges, O.V. Naumenko, O.L. Polyansky, L.S. Rothman, R.A. Toth, A.C. Vandaele, N.F. Zobov, A.Z. Fazliev, T. Furtenbacher, I.E. Gordon, S.N. Mikhailenko, B.A. Voronin, J. Quant. Spectrosc. Rad. Transf. 111 (2010) 2160–2184.
[29] L.S. Rothman, I.E. Gordon, A. Barbe, D.C. Benner, P.F. Bernath, M. Birk, V. Boudon, L.R. Brown, A. Campargue, J.-P. Champion, K. Chance, L.H. Coudert, V. Dana, V.M. Devi, S. Fally, J.-M. Flaud, R.R. Gamache, A. Goldman, D. Jacquemart, I. Kleiner, N. Lacome, W.J. Lafferty, J.-Y. Mandin, S.T. Massie, S.N. Mikhailenko, C.E. Miller, N. Moazzen-Ahmadi, O.V. Naumenko, A.V. Nikitin, J. Orphal, V.I. Perevalov, A. Perrin, A. Predoi-Cross, C.P. Rinsland, M. Rotger, M. imekov, M.A.H. Smith, K. Sung, S.A. Tashkun, J. Tennyson, R.A. Toth, A.C. Vandaele, J.V. Auwera, J. Quant. Spectrosc. Radiat. Transf. 110 (2009) 533–572.